

Assessment of the Woodford Shale Petroleum System Within a Deep Subbasin on the Central Basin Platform, Permian Basin*

William R. Drake¹, Mark W. Longman¹, and Andrew Moses¹

Search and Discovery Article #11105 (2018)**

Posted July 23, 2018

*Adapted from extended abstract prepared in conjunction with oral presentation given at AAPG 2018 AAPG Annual Convention and Exhibition, Salt Lake City, Utah, May 20-23, 2018

**Datapages © 2018 Serial rights given by author. For all other rights contact author directly.

¹QEP Resources, Inc., Denver, Colorado, United States (william.drake@qepres.com)

Abstract

The thickest and most distal section of the Upper Devonian Woodford Shale in the Permian Basin was deposited near the axial depocenter of the early to mid-Paleozoic Tobosa Basin. Today, a >560 foot thick section of the Woodford is preserved in a subbasin on the Permian Basin's Central Basin Platform (CBP). Conventional core was cut from 11,468 to 11,515 feet TVD in northwestern Winkler County, Texas to define the geologic properties of the Woodford at this location and assess its viability as an unconventional resource play. A full suite of core, log, and cuttings data is used to characterize rock compositions, facies, reservoir properties, and thermal maturity. The Woodford at this location is an organic-rich, slightly dolomitic, silty, pyritic, highly-siliceous mudstone, averaging 55-75% silica, 10-30% detrital clay, and 5-9 weight% TOC. Thin-section analysis of the core reveals three main facies: pyritic radiolarian chert, radiolarian-poor siliceous mudstone, and mixed chert-mudstone.

Trace element data from over the full Woodford section suggest dramatic changes in basin restriction through time, possibly recording a second-order sea level highstand during the early Frasnian followed by regression and overprinting by higher-order cycles through the latest Famennian. Porosity ranges from 6-10%, and permeability was measured in the nanodarcy range, with oil and water saturations averaging >47% and <25%, respectively. Rock pyrolysis, oil extract, oil biomarkers, and gas isotopes indicate that thermal maturity ranges from 0.91-0.94 %Ro equivalent, indicating late peak-oil generation with little migration. We use a strong depth-maturity relationship to demonstrate that the entire subbasin area is within the oil generation window.

High inorganic porosity filled with organic matter and common organic-hosted nanoporosity is visible in FE-SEM images. High magnification images reveal that most of the Woodford's silica-rich matrix consists of silica nanospheres 200-500 nm in diameter interpreted to have formed penecontemporaneously with deposition and preventing formation compaction through time. The sum of our findings indicates that the thick, distal Woodford Shale section in the Winkler County subbasin has key attributes required to be a viable source-rock reservoir, whereas the Woodford elsewhere on the CBP typically lacks thickness and/or adequate thermal maturity.

Introduction

The Woodford Shale in the Permian Basin of West Texas and southeastern New Mexico consists predominantly of black, organic-rich siliceous mudstone with chert, siltstone, and dolomite (e.g., Comer, 1991; Hemmesch et al., 2014), and was deposited at the peak of a 2nd-order, marine eustatic high reached in the Frasnian Stage of the Upper Devonian (Haq and Schutter, 2008) ([Figure 1](#)). The formation is a prolific source rock in Oklahoma, West Texas, and New Mexico, but it is a proven horizontal drilling target and oil producer only in Oklahoma ([Figure 2](#)). This leads to the question of why the viable oil window Woodford play is elusive in the Permian Basin. A simple answer is that in the Delaware Basin, the Woodford is typically deep, in the dry gas window, or subject to migrated gas where rock maturity is in the oil window. In the Midland Basin, the Woodford is relatively thin and typically in or near the gas window. Along the Central Basin Platform (CBP), the Woodford is thickest where the section is complete, between structural uplifts, but often lacks adequate thermal maturity. A thick section in the oil window, however, can be found flanking the western edge of the CBP and in deep structural subbasins on the CBP. This study focuses on a section of the Woodford preserved in a deep subbasin on the CBP in an area previously considered marginally mature. The purpose of this assessment is to define the geologic properties of the Woodford in a deep structural subbasin in northwestern Winkler County, Texas and assess its viability as an unconventional resource play.

Woodford Shale on the Central Basin Platform

The Woodford Shale was deposited in the ancestral Tobosa Basin, the precursor to the modern Permian Basin, where the thickest section accumulated along the axial depocenter of the basin ([Figure 2](#)). Superimposing the Woodford depositional thickness over the Permian Basin shows that the thickest, most distal section of the Woodford is mainly positioned over the CBP, where depositional thickness exceeded 600 ft (183 m). A variable thickness was deposited over the future Delaware Basin, and the thinnest section was deposited over the future Midland Basin ([Figure 2](#)). A West-East cross section over the central Permian Basin shows uplift of the CBP relative to the Delaware and Midland basins ([Figure 3](#)). An erosional truncation of mid-to-late Paleozoic section at the lower Permian unconformity exists on the CBP, but Pennsylvanian and older section is preserved in structural lows. The present-day isochore of the Woodford in the northern Winkler County, TX area reveals this rapid thinning due to the unconformity and uplift on large reverse faults along the CBP ([Figure 3](#)). The thickest Woodford section is preserved between uplifted fault blocks and the erosional subcrop, where it ranges from approximately 500 to 650 ft (150 to 200 m) thick ([Figure 4](#)). The regional depth-structure map for this area shows the presence of a deep subbasin in northwestern Winkler County where the top Woodford is over 11,500 ft (3,500 m) deep ([Figure 5](#)). Several early horizontal Woodford wells are in the area and, despite short lateral lengths and understimulation relative to current standards, they all produced sufficient quantities of oil to suggest that a working petroleum system is in place. Thermal maturity of the Woodford in this area ranges from 0.51 to 0.69%Ro (including both measured vitrinite reflectance and calculated %Ro from Tmax). Previous to this evaluation, the only thermal maturity data point from the subbasin of northwestern Winkler County came from the Goff #1 well ([Figure 5](#)), where vitrinite reflectance (measured) was reported as 0.55%Ro. However, this represents an unreliable data point based on the use of cuttings over a 590 ft (180 m)-thick interval, problematic visual analysis of “super fine amorphous kerogen”, and the combining of three vitrinite populations into one histogram to arrive at the reported Ro value. In order to better assess the viability of the Woodford Shale as a source-rock reservoir and horizontal target in this subbasin, uncertainties in important geologic properties such as thermal maturity and rock composition must be resolved.

Data Acquisition

To characterize and evaluate the geologic properties of the Woodford Shale in this subbasin on the CBP, the Hentz Family 7-1 pilot well was drilled in a deep portion of the subbasin in northwestern Winkler County ([Figure 5](#)) with the primary objective of defining depths, facies, saturations, organic richness, rock properties, and thermal maturity. Conventional core was cut from 11,468 to 11,515 feet TVD and covers a 47 ft (14 m) portion of the upper Woodford section ([Figure 6](#)). Coverage of open-hole logs and cuttings samples extended through the Pennsylvanian section to the Devonian limestone below the Woodford Shale ([Figure 6](#)). Data from core samples are from X-ray fluorescence (XRF), X-ray diffraction (XRD), source-rock analysis (SRA), crushed-rock analysis (GRI), thin-section petrography, field emission scanning electron microscopy (FE-SEM), and source-rock extract analysis. Cuttings analyses included XRF, XRD, and SRA. Production oil and head-space gas from core tubes were also analyzed for comparison to core properties.

Results and Discussion

Rock Properties

The Woodford Shale in northwestern Winkler County is an organic-rich, slightly dolomitic, silty, pyritic, highly-siliceous mudstone, averaging 55-75% silica, 10-30% detrital clay, and 5-9 wt% TOC. Thin-section analysis with a light petrographic microscope reveals three main facies that comprise the core: pyritic radiolarian chert, radiolarian-poor siliceous mudstone, and mixed chert and mudstone ([Figure 7](#), [Figure 8](#), and [Figure 9](#)). The facies can be identified in context to the spectral gamma ray log from the core ([Figure 10](#)), which shows uranium as the dominant control on the total gamma ray response.

The GRI results for samples from along the core yielded averages in porosity of 8.1%, water saturation of 25%, and oil saturation of 47.7% ([Figure 11](#)). Note that TOC closely tracks both porosity and oil saturation, and it increases with depth along with the higher gamma-ray response. Water saturation, in contrast, appears inversely correlated with this trend and drops below 15% at the base of the core where the gamma ray is highest. Results from XRD analysis yielded averages in quartz of 65.5%, clay of 23.3%, dolomite of 2.7%, and pyrite of 3.9% ([Figure 12](#)). Pyrite percentage generally tracks TOC richness, while clay inversely correlates with quartz content. Near the base of the core, where oil saturation and porosity are highest, the percentage of quartz exceeds 75% with clay percentage dropping below 12%.

FE-SEM Imaging

We used FE-SEM on argon ion-milled surfaces to identify the primary constituents and to characterize the texture of the Woodford core ([Figure 13](#) and [Figure 14](#)). Listed in order of decreasing abundance, silica components are: 1) newly-identified silica nanospheres (200-500 nm in diameter); 2) radiolarians; 3) detrital quartz silt; 4) unidentified micron-sized microfossils; and 5) sponge spicules (Drake et al., 2017). The silica nanospheres comprise two to four times all other forms of silica combined (Longman et al., in press), indicating that the silica nanospheres are the primary constituent of the Woodford Shale at this location. When viewed at high magnification, the Woodford matrix is commonly characterized by a “cloudy” texture where milled surfaces crosscut through nanosphere aggregates and interparticle pores ([Figure](#)

[13](#)). Note that in the area of ion-milled nanospheres and pore space, euhedral crystals of authigenic quartz appear as overgrowths on and between silica nanospheres, signifying that the nanospheres were present before the formation of quartz overgrowths rather than the converse. The nanospheres appear to have formed penecontemporaneously with deposition and as a cement that helped prevent compaction of the rock matrix (Longman et al., in press). Further, they may be a product of microbial activity that also possibly played a role in creating anoxic bottom-water conditions that promoted the preservation of the organic matter.

Trace Elements and Basin Restriction

Although the conditions that promoted the formation of silica nanospheres is still an area of active research, possible controls on the sea-floor environment during Woodford time could have been the degree of basin (or hydrographic) restriction and cycles of benthic redox potential. Algeo and Lyons (2006) and Algeo et al. (2007) used the covariance of molybdenum (Mo) and TOC as a first-order indicator of basin restriction and eustatic and/or tectonic changes. They link a low Mo/TOC ratio to a limited deepwater resupply of Mo, which suggests a restricted or silled basin during low sea-level stands. In contrast, they relate a high Mo/TOC ratio to enhanced deepwater renewal of Mo (i.e., increased connectedness to undepleted open ocean), which suggests a weakly-restricted basin during high sea-level stands and open-marine conditions.

At the Hentz Family 7-1, concentrations of Mo (from XRF) and TOC were determined from cuttings collected over entire Woodford section ([Figure 6](#)). The plot of the Woodford data suggests cycles of sea-level shallowing and basin restriction (silling) from which anoxic conditions can be inferred ([Figure 15](#)). According to Haq and Schutter (2008) and Hemmesch et al. (2014), a second-order sea level highstand took place during the early Frasnian and was followed by an overall regression through the latest Famennian. Overprinting by higher-order cycles has been proposed for the Woodford Shale in the Permian Basin (Hemmesch et al. 2014). The cycles of Mo/TOC from the Hentz Family 7-1 Woodford section appear to record the maximum second-order sea-level highstand in the early Frasnian, as well as the end-Devonian transgression and eustatic event of Algeo et al. (2007) ([Figure 15](#)). Higher-order cycles of Mo/TOC are evident throughout the Woodford section. Although the methodology above has limitations for our study, such as loss of TOC and the enrichment of Mo due to thermal maturation, the oscillations of Mo/TOC nevertheless hint at important marine cycles.

Further evidence of basin shallowing comes from oil biomarkers such as carotenoids, which can be useful in predicting water depths (i.e., light penetration) during source-rock deposition. Paleoisorienaterane was detected in Woodford oil from the Bruce & Bar A55A56-2303 N 02WS (adjacent horizontal well, same landing zone as the Hentz Family 7-1H). The presence of the biomarker suggests highly anoxic shallow waters during source-rock deposition (aka photic zone euxinia) (Sinninghe Damsté et al., 1993) in a restricted, semi-enclosed basin (e.g., Sluijs et al., 2014), despite the distalmost and presumably deepest portion of the former Tobosa Basin.

Thermal Maturity: Source Rock, Oil, and Gas

Source-rock analysis was conducted on 17 evenly-spaced samples along the core, and the key results are summarized on [Table 1](#). Tmax averages 448, which converts to approximately 0.91 calculated %Ro (after Jarvie, et al., 2001), indicating that the Woodford at this location is in the peak oil-generation window. The hydrogen indices vs Tmax values suggest that the Woodford kerogen is oil-prone Type II ([Figure 16](#)),

consistent with previous reports (e.g., Comer, 1991; Parker et al., 2014). Analysis of four additional core samples associated with source-rock extraction analysis also yielded the same average calculated %Ro of 0.91 ([Table 2](#)).

Oil samples were analyzed using the GC-triple quadrupole mass spectrometer to determine the lighter/mid-range maturity based on thermally-dependent C11-C18 alkyl aromatic ratios (VREQ) (GeoMark methodology: Rocher et al., 2015). Results for core-extract samples (0.93 to 0.94 VREQ) are very similar to results for produced oil samples (approximately 0.94 VREQ) ([Table 2](#)). Gas maturity based on ethane and propane carbon isotopes (VREG) (GeoMark proprietary isotope/maturity calibration scale) averages approximately 0.93 for core head-space samples ([Table 2](#)). The low asphaltenes sulfur, and average saturates/aromatics ratio all confirm high quality oil and are consistent with the API gravity of 42.0 deg.

Together, all maturity data for source-rock, oil, maturities are very similar, suggesting minimal or no migration of oil and gas. The new maturity data along with other Tmax data from the region exhibit a strong depth-to-thermal-maturity relationship that can be used to transform depth-structure to a maturity map ([Figure 17](#)). The regional thermal-maturity map indicates that the whole region is within the early oil window, but only the subbasin is within the peak oil-generation window.

Conclusions

New core data and oil and gas analytical results for northwestern Winkler County, Texas define the geologic properties of the Woodford in a deep structural subbasin in northwestern Winkler County, Texas. The thick (>560 ft), distal Woodford Shale section at this location is an organic-rich, slightly dolomitic, silty, pyritic, siliceous mudstone. Core and cuttings analyses confirm favorable rock compositions and TOC, facies, reservoir properties, thermal maturity, and saturations:

Woodford Shale (Hentz Family 7-1)						
Silica	Clay	TOC (wt)	Porosity	Calc. %Ro*	S _o	S _w
55-75%	15-30%	5-9%	8-10%	0.91-0.94	>50%	<20%

*after Jarvie et al., 2001

High magnification FE-SEM images reveal that most of the Woodford’s silica-rich matrix consists of authigenic silica nanospheres (200-500 nm in diameter), which are interpreted to have formed penecontemporaneously with deposition and to have minimized formation compaction through time. Oscillating Mo/TOC ratios suggest tectonic and/or eustatic sea-level changes, variable degrees of basin restriction, and cycles in redox potential during Woodford deposition. All these cycles could have broadly contributed first-order controls on observed rock composition and the preservation of organic carbon.

Thermal maturity from oil, source-rock extract, and gas analyses are consistent with rock pyrolysis data and confirm that the Woodford at this location 1) is in the peak oil-generation window, 2) is low in asphaltenes, and 3) produces high oil quality. A strong depth-to-thermal-maturity

relationship demonstrates that the entire subbasin area is within the peak oil-generation window. The area of ≥ 0.85 %Ro (calculated) covers approximately 50,000 acres and suggests the potential for an oil-window resource play of modest scale. The Woodford elsewhere on the CBP, however, commonly lacks its original depositional thickness and/or adequate thermal maturity to be a viable horizontal target in the peak oil window.

Acknowledgments

We thank QEP Resources for permission to publish this work, and Core Lab, GeoMark, and Weatherford Labs for high-quality laboratory support.

References Cited

Algeo, T.J. and T.W. Lyons, 2006, Mo–Total Organic Carbon Covariation in Modern Anoxic Marine Environments: Implications for Analysis of Paleoredox and Paleohydrographic Conditions: *Paleoceanography*, v. 21, PA1016. <https://doi.org/10.1029/2004PA001112>. Website accessed July 2018.

Algeo, T.J., T.W. Lyons, R.C. Blakey, and D.J. Over, 2007, Hydrographic Conditions of the Devonian-Carboniferous North American Seaway Inferred from Sedimentary Mo-TOC Relationships: *Palaeogeography, Palaeoclimatology, Palaeoecology*, v. 256, p. 204-230. <https://doi.org/10.1016/j.palaeo.2007.02.035>. Website accessed July 2018.

Comer, J.B., 1991, Stratigraphic Analysis of the Upper Devonian Woodford Formation, Permian Basin, West Texas and Southeastern New Mexico: Report of Investigations No. 201, Bureau of Economic Geology, University of Texas at Austin, 63 p.

Drake, W.R., M.W. Longman, and J. Kostelnik, 2017, The Role of Silica Nanospheres in Porosity Preservation in the Upper Devonian Woodford Shale on the Central Basin Platform, West Texas: RMAG/DWLS Fall Symposium: Geology and Petrophysics of Unconventional Mudrocks, Golden, CO, September 27, 2017, p. 135-146.

Haq, B.U., and S.R. Shutter, 2008, A Chronology of Paleozoic Sea-Level Changes: *Science*, v. 322, p. 64-68. <https://doi.org/10.1126/science.1161648>. Website accessed July 2018.

Hemmesch, N.T., N.B. Harris, C.A. Mnich, and D. Selby, 2014, A Sequence-Stratigraphic Framework for the Upper Devonian Woodford Shale, Permian Basin, West Texas: *American Association of Petroleum Geologists Bulletin*, v. 98, p. 23-47. <https://doi.org/10.1306/05221312077>. Website accessed July 2018.

Jarvie, D.M., B.L. Claxton, B. Henk, and J.T. Breyer, 2001, Oil and Shale Gas from the Barnett Shale, Ft. Worth Basin, Texas: AAPG National Convention, June 3-6, 2001, Denver, CO, *American Association of Petroleum Geologists Bulletin*, v. 85/13 (Supplement), p. A100.

Longman, M.W., K.L. Milliken, T.M. Olson, and W.R. Drake, in press, A Comparison of Silica Diagenesis in the Devonian Woodford Shale (Central Basin Platform, West Texas) and Cretaceous Mowry Shale (Powder River Basin, Wyoming), *in* W. Camp et al. (eds), AAPG Memoir: Mudstone Diagenesis: New Research Perspectives for Shale Hydrocarbon Reservoirs, Seals, and Source Rocks.

Matchus, E.J., and T.S. Jones, 1984, East–West Cross Section Through Permian Basin of West Texas: West Texas Geological Society Publication 84-79, 1 p.

Parker, A., D. Entzminger, J. Leone, M. Sonnenfeld, and L. Canter, 2014, Lessons Learned from the KCC #503H Woodford Horizontal Well at Keystone South Field, Winkler County, TX: AAPG 2014 Southwest Section Annual Convention, Midland, Texas, May 11-14, 2014, [Search and Discovery Article #20254 \(2014\)](#). Website accessed July 2018.

Rocher, D., J. Zumberge, and J. Curtis, 2015, Estimating Thermal Maturity of Light Oils and Condensates – VREQ Using GC-Triple Quad MS to Measure Alkyl Aromatics, etc.: GeoMark Research in-house workshop, June 15, 2015, 13 p.

Ryan, W.B.F., S.M. Carbotte, J.O. Coplan, S. O'Hara, A. Melkonian, R. Arko, R.A. Weissel, V. Ferrini, A. Goodwillie, F. Nitsche, J. Bonczkowski, and R. Zemsky, 2009, Global Multi-Resolution Topography Synthesis: Geochemistry, Geophysics, Geosystems, v. 10, Q03014. <http://dx.doi.org/10.1029/2008GC002332>. Website accessed July 2018.

Sinninghe Damsté, J.S., S.G. Wakeham, M.E.L. Kohnen, J.M. Hayes, and J.W. de Leeuw, 1993, A 6,000-Year Sedimentary Molecular Record of Chemocline Excursions in the Black Sea: *Nature*, v. 362, p. 827-829. <http://dx.doi.org/10.1038/362827a0>. Website accessed July 2018.

Sluijs, A., L. Van Roij, G.J. Harrington, S. Schouten, J.A. Sessa, L.J. LeVay, G.J. Reichart, and C.P. Slomp, 2014, Warming, Euxinia and Sea Level Rise During the Paleocene-Eocene Thermal Maximum on the Gulf Coastal Plain: Implications for Ocean Oxygenation and Nutrient Cycling: *Climate of the Past*, v. 10, p. 1421-1439. <http://dx.doi.org/10.5194/cp-10-1421-2014>. Website accessed July 2018.

Wright, W.F., 1979, Petroleum geology of the Permian Basin: West Texas Geological Society Special Publication, 98 p.

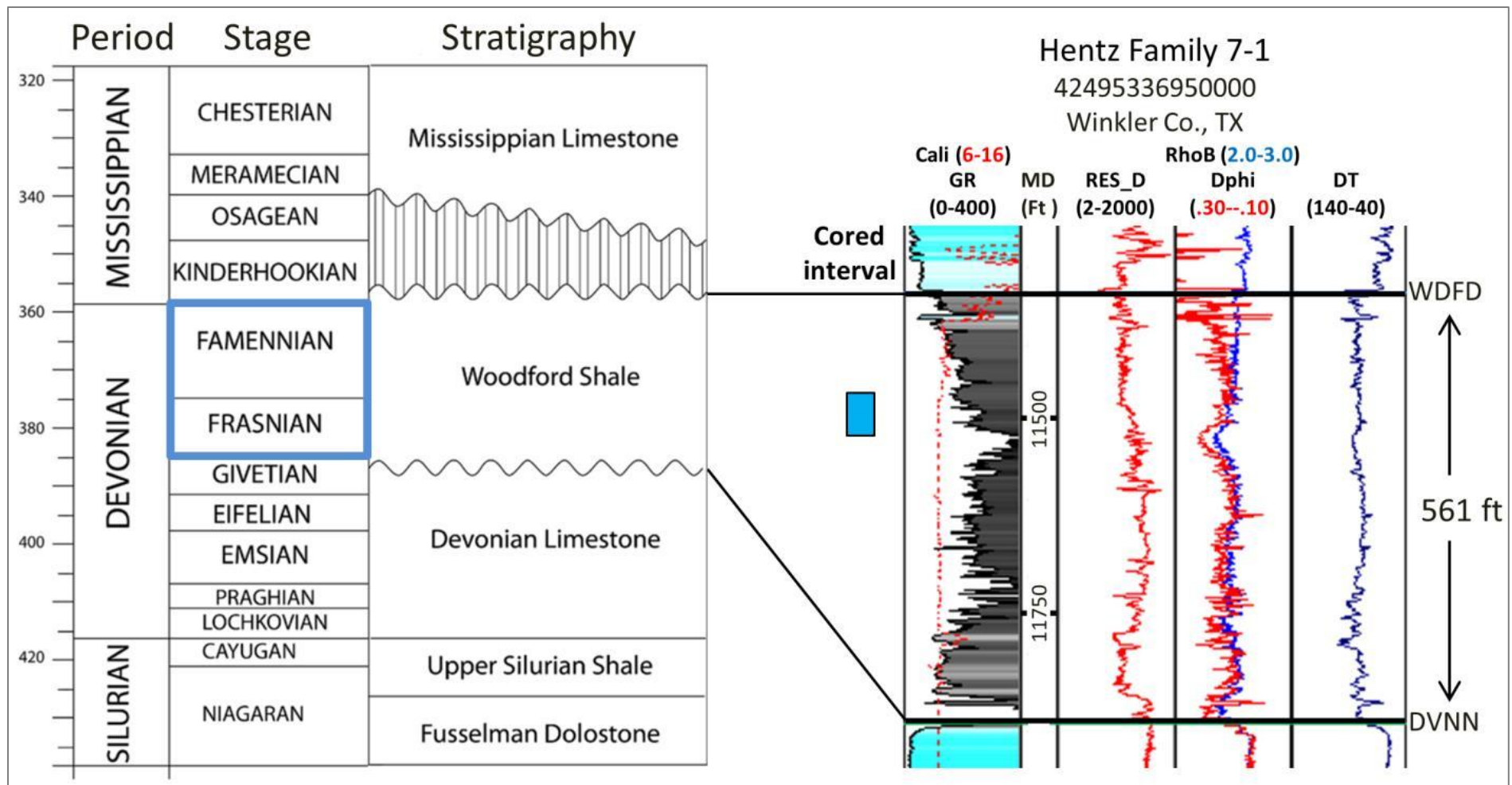


Figure 1. Age of the Woodford Shale in the Permian Basin (modified from Hemmesch et al., 2014, after Comer, 1991). Location of Hentz Family 7-1 is shown on [Figure 2](#). Abbreviations: Cali - caliper, GR - gamma ray, MD - measured depth, Res_D - deep resistivity, RhoB - bulk density, Dphi - density porosity, DT - sonic, WDFD - Woodford Shale, DVNN - Devonian limestone.

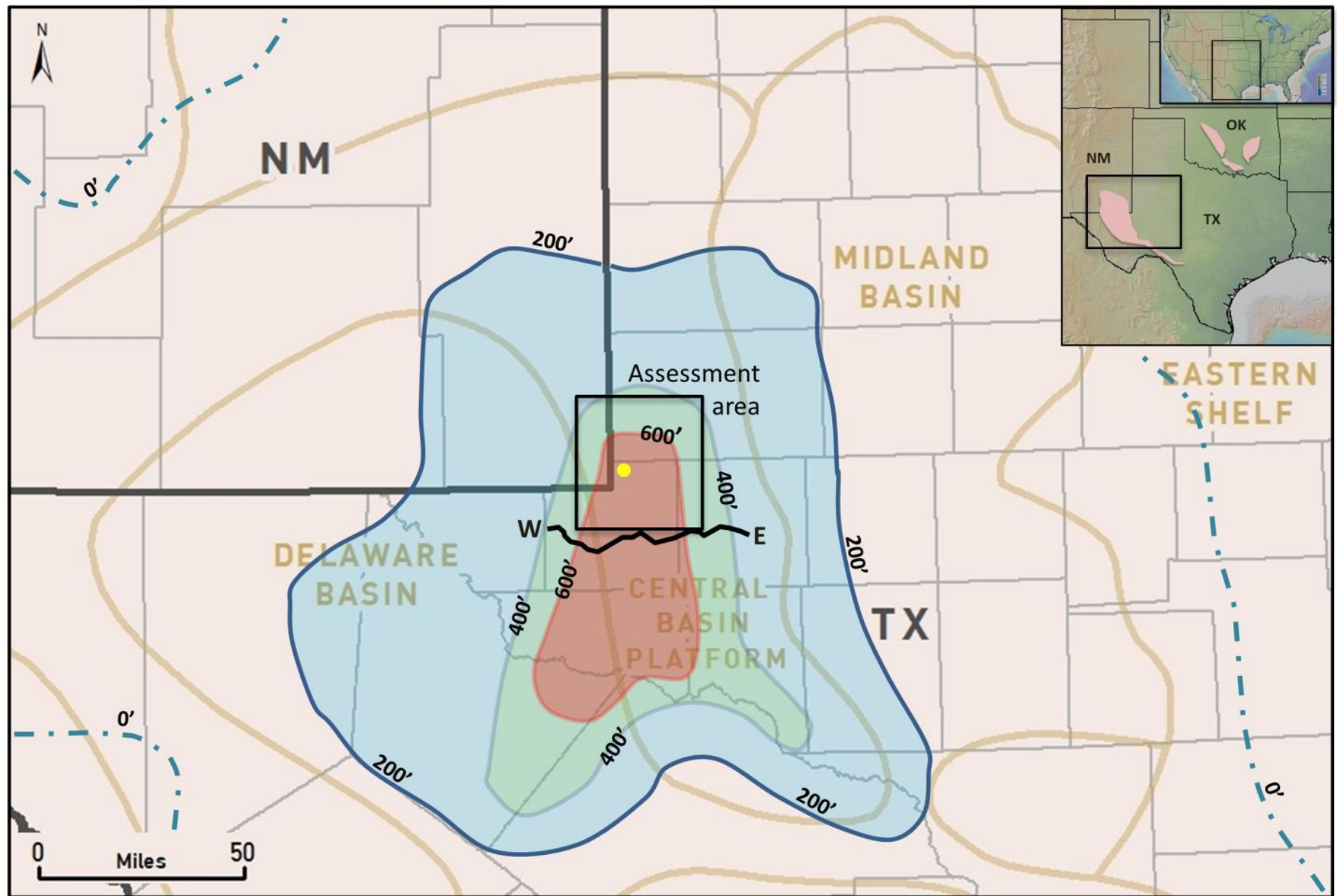


Figure 2. Woodford Shale depositional thickness (adapted from Wright, 1979) superimposed over the modern Permian Basin. Yellow dot marks the location of the Hentz Family 7-1 well. W-E cross section is presented on Figure 3. Pink regions on inset map are the main areas of Woodford production (Inset map: <http://www.geomapp.org>; Ryan et al., 2009).

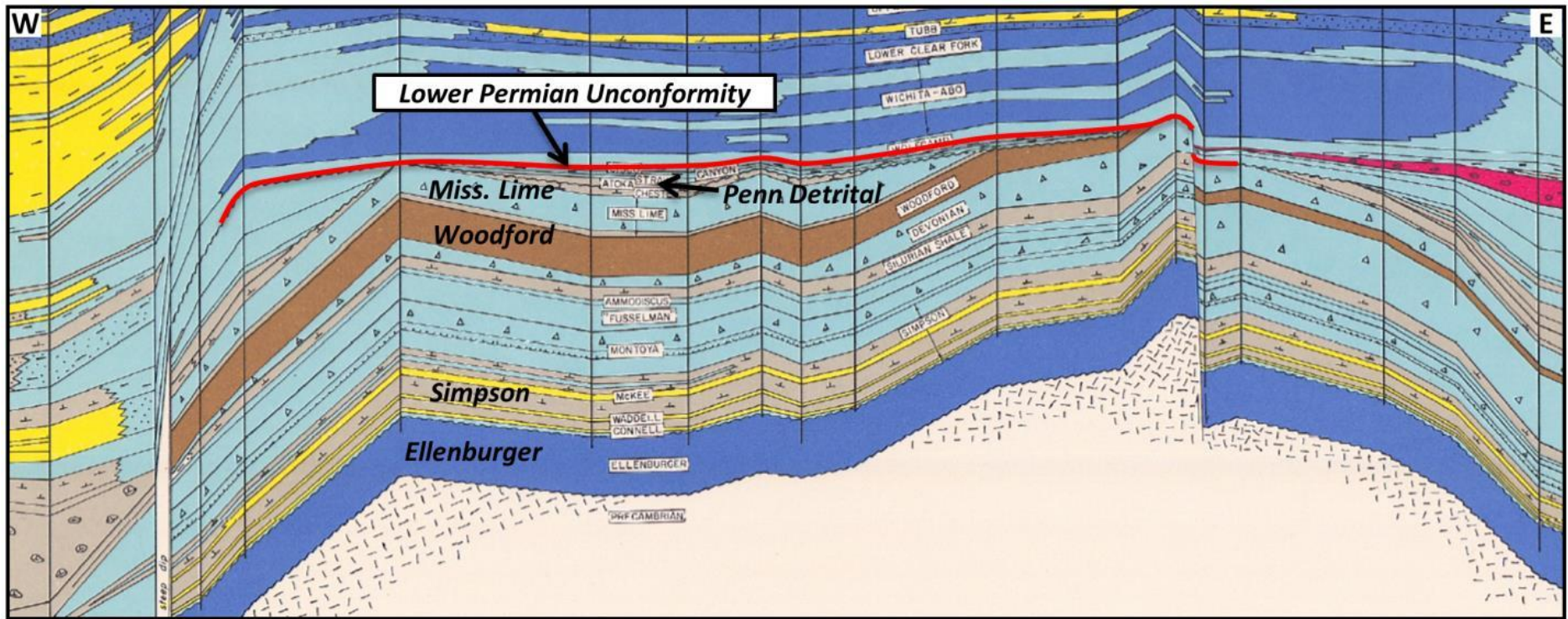


Figure 3. West-East structural cross section from the eastern Delaware Basin to the western Midland Basin (see [Figure 2](#)) (modified from Matchus and Jones, 1984). Vertical exaggeration = 10.5:1.

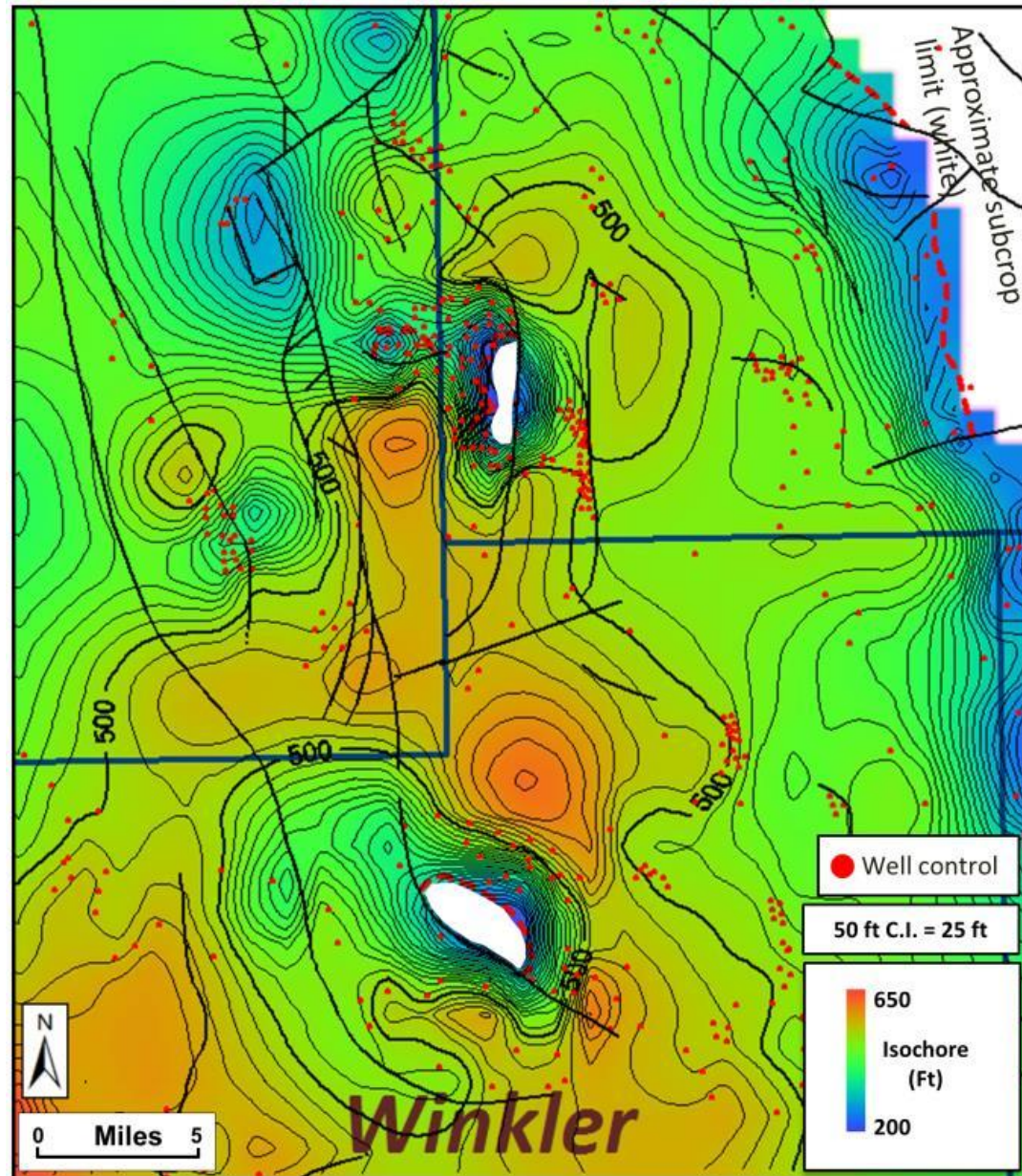


Figure 4. Woodford Shale isochore with mapped faults.

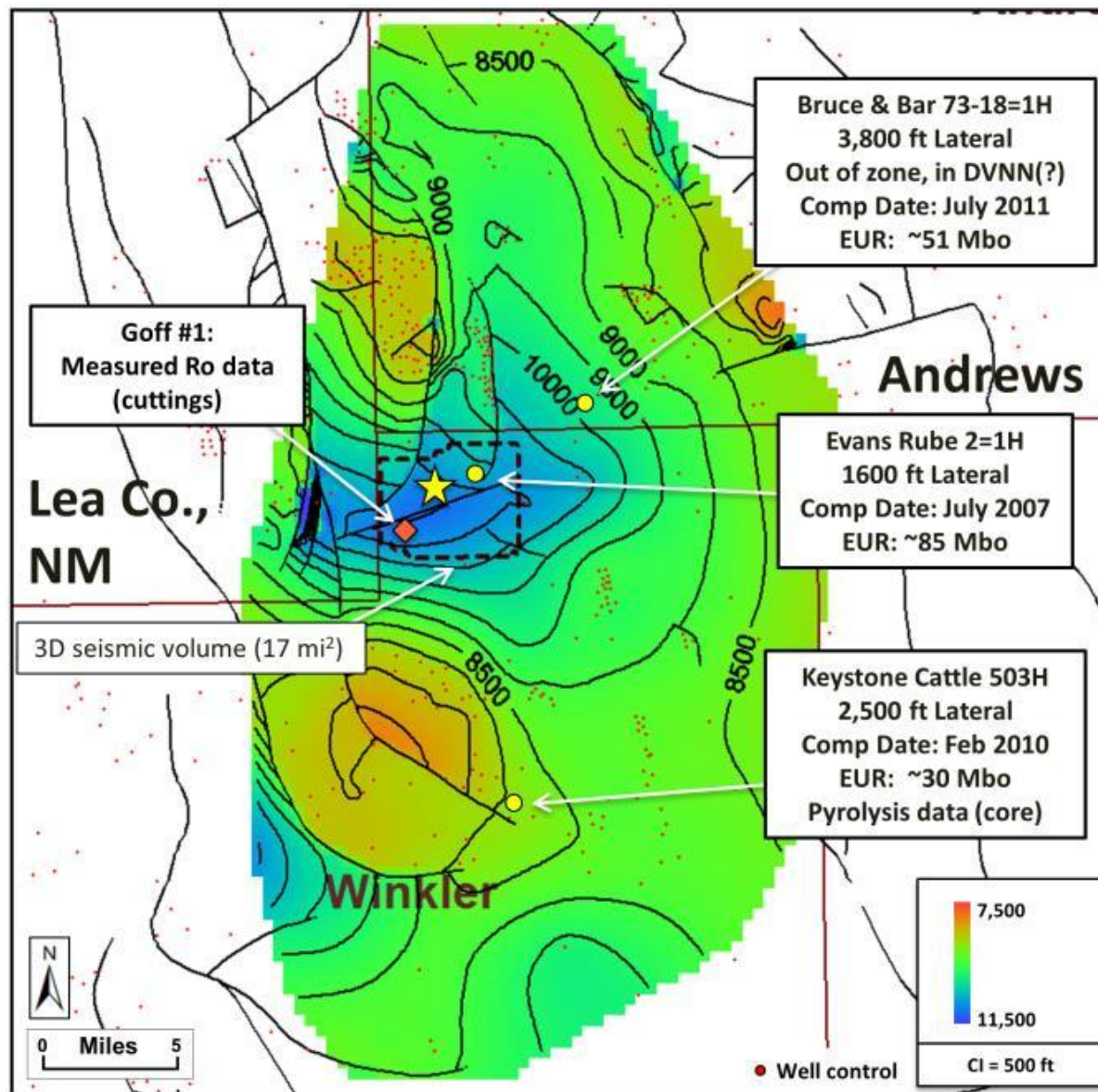


Figure 5. Woodford regional depth-structure map with producing horizontal wells. Yellow star = Hentz Family 7-1.

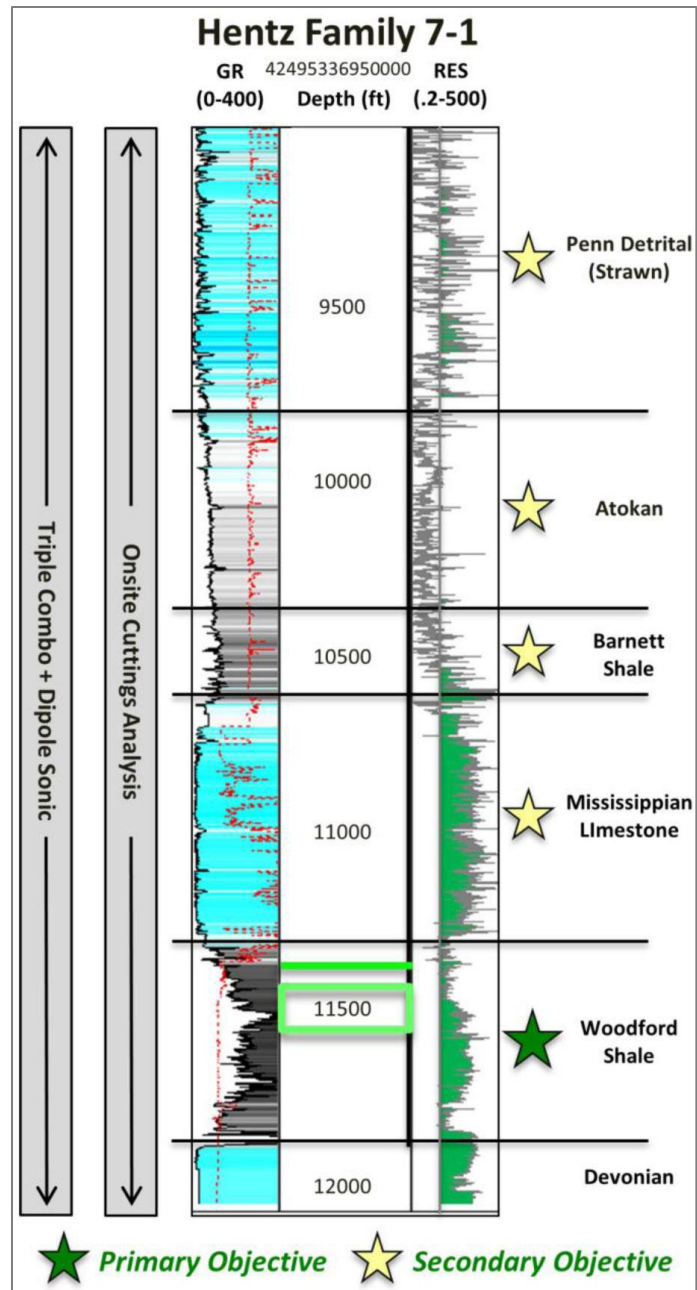


Figure 6. Data acquisition at the Hentz Family 7-1. Cored interval is from 11,468 to 11,515 ft TVD (neon green box).

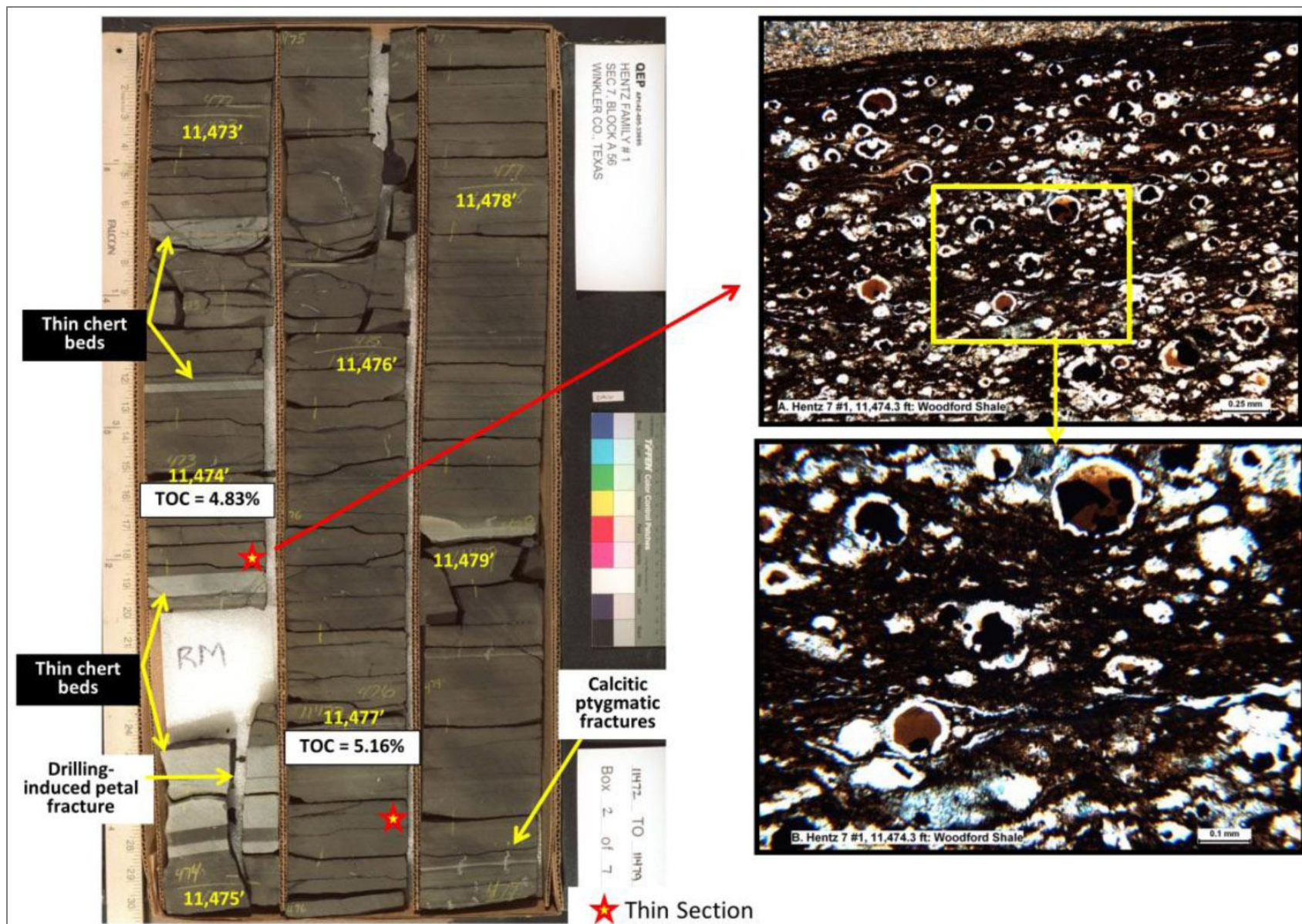


Figure 7. Core image and thin-section photomicrograph of Facies 1: pyritic radiolarian chert.

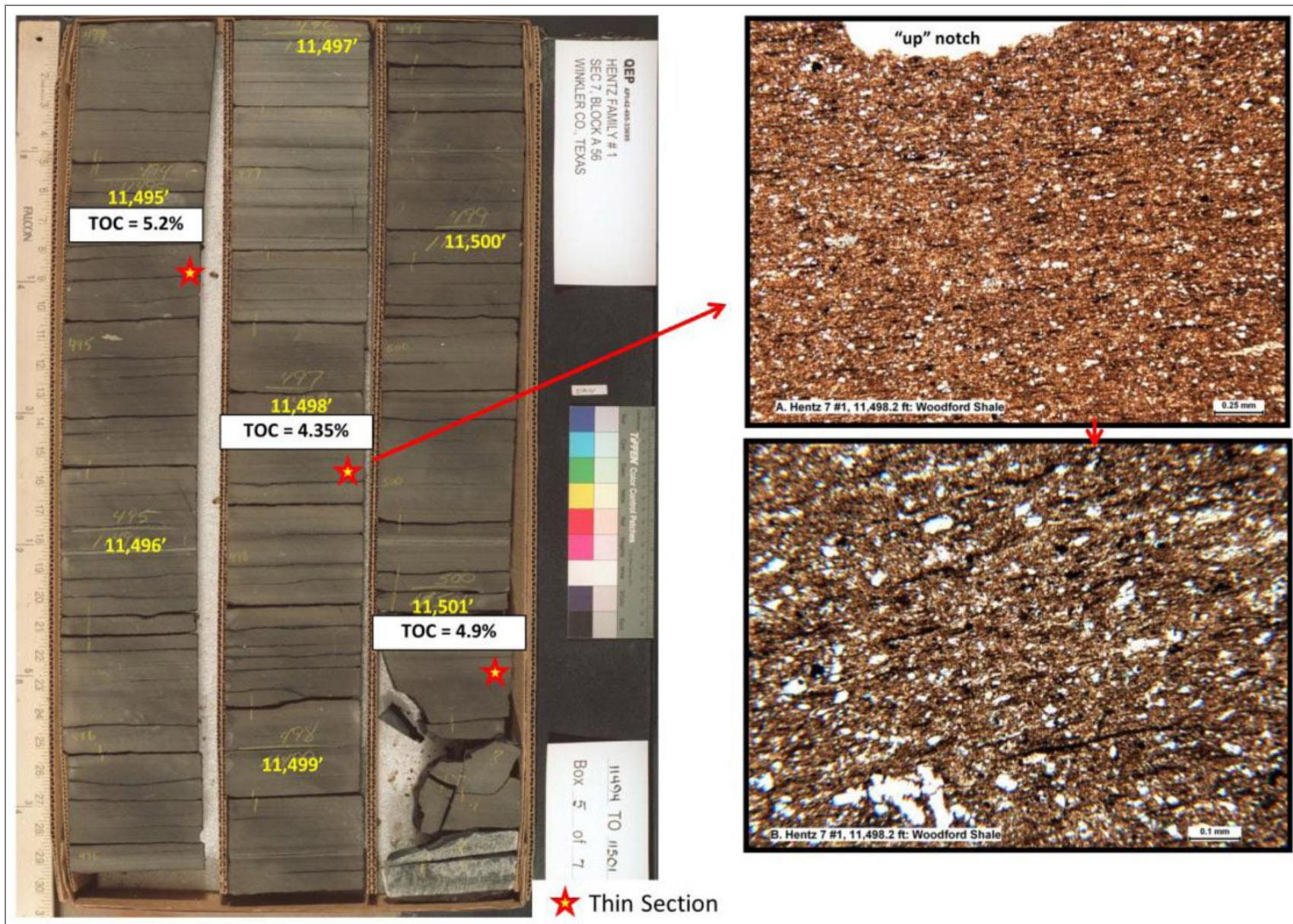


Figure 8. Core image and thin-section photomicrograph of Facies 2: radiolarian-poor siliceous mudstone.

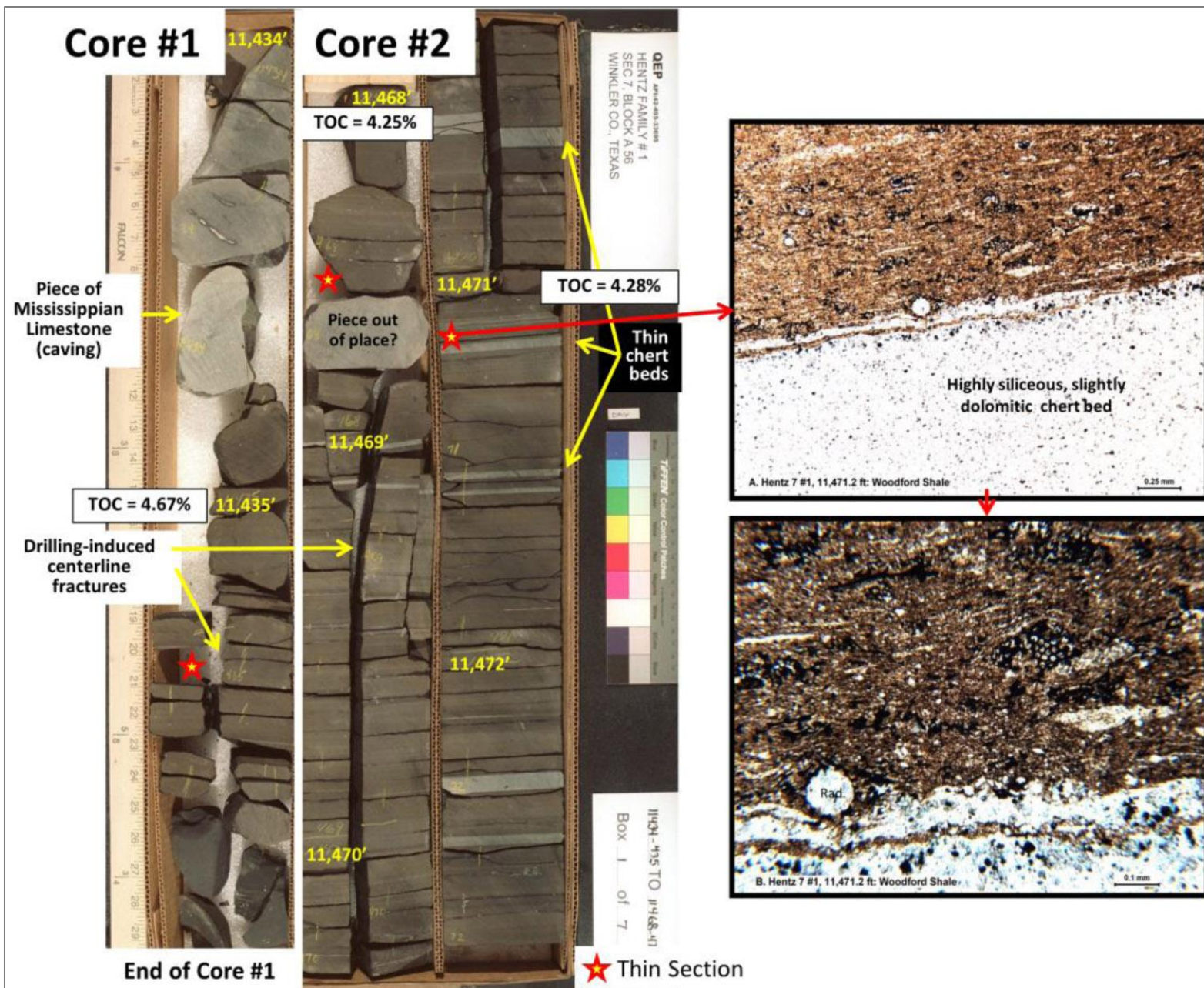


Figure 9. Core image and thin-section photomicrograph of Facies 3: mixed chert and mudstone.

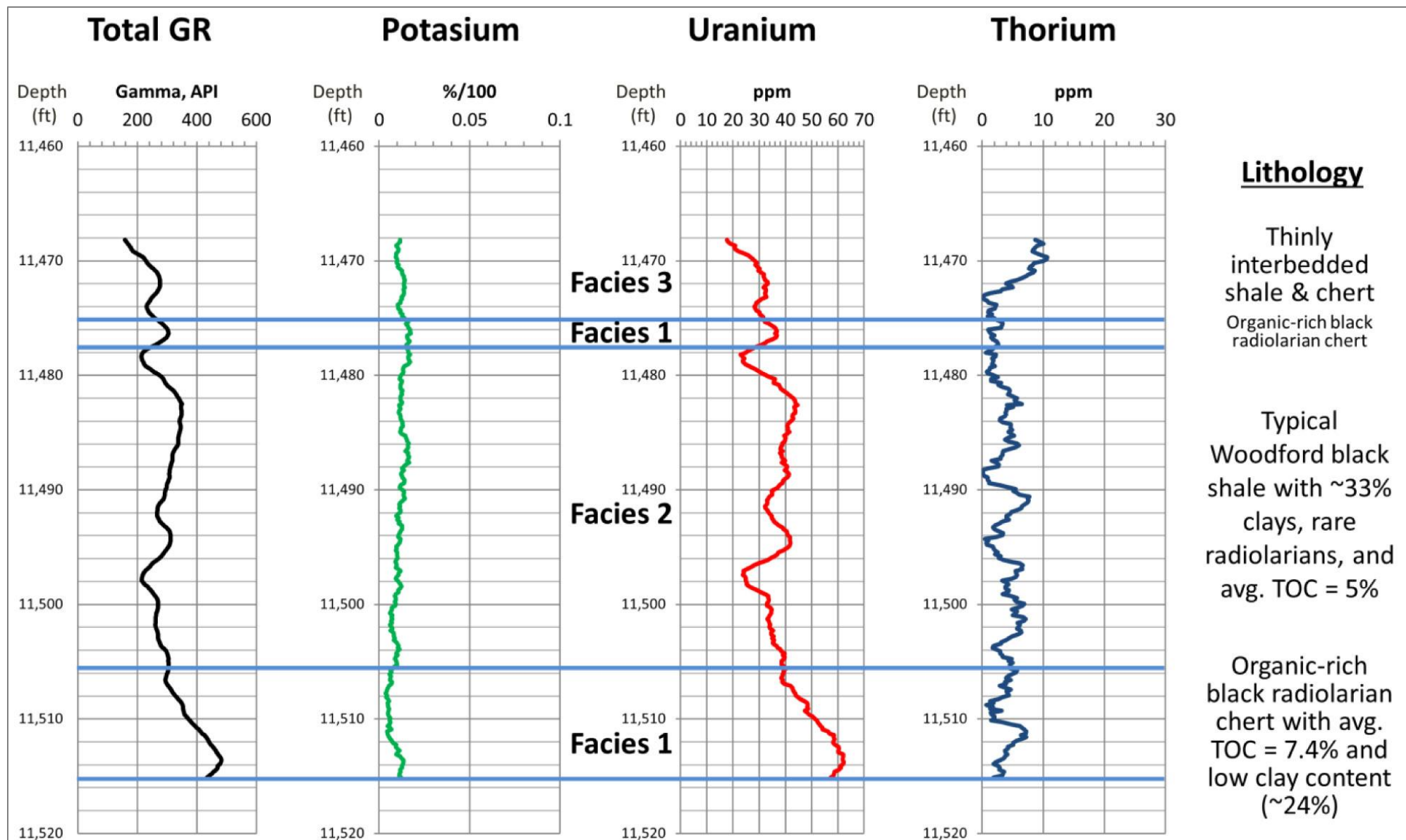


Figure 10. Spectral gamma-ray logs for Woodford Shale core from the Hentz Family 7-1.

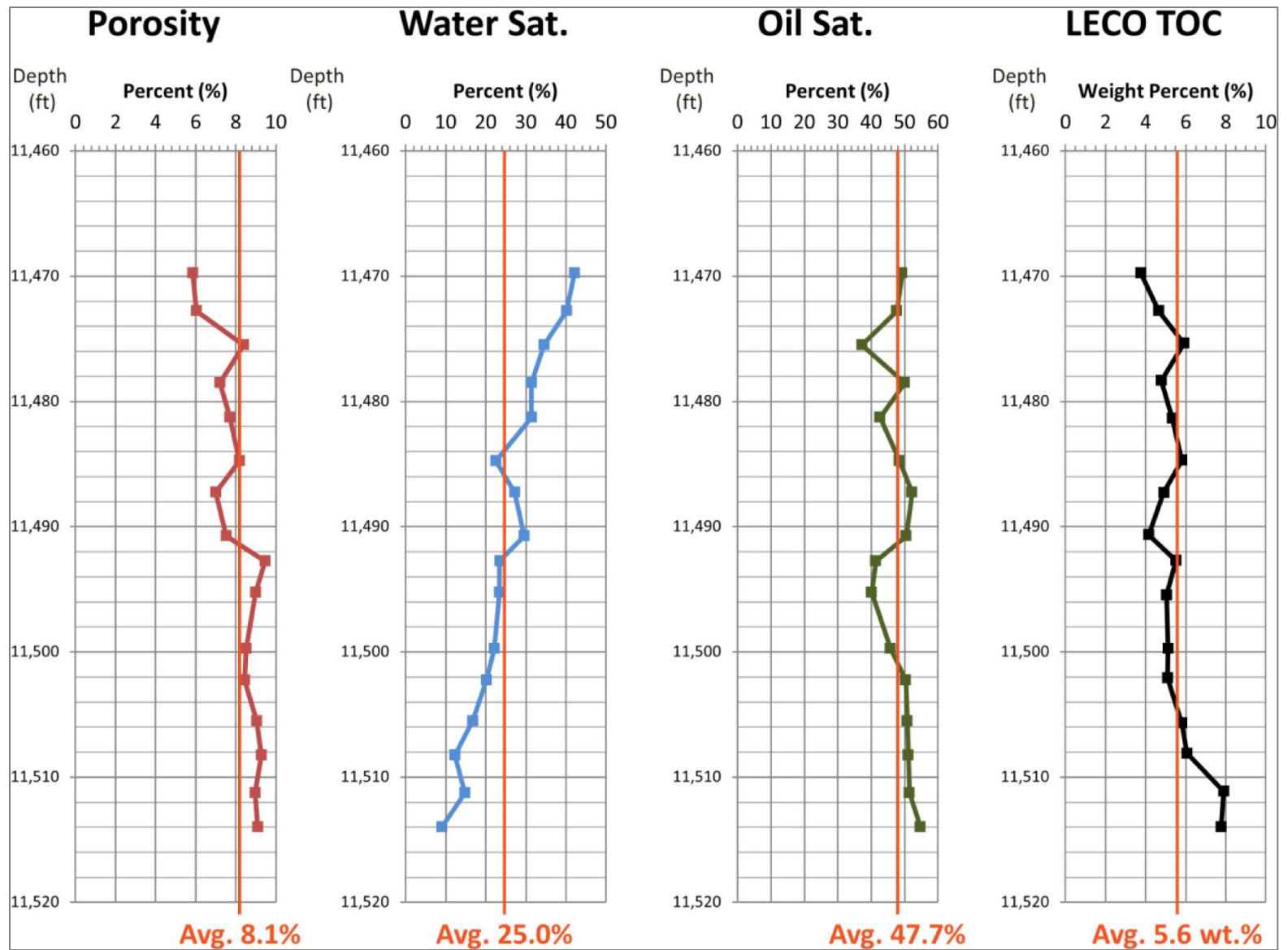


Figure 11. Crushed rock (GRI) and TOC results for the Woodford Shale core from the Hentz Family 7-1. GRI analyses are from dry and Dean Stark extracted conditions.

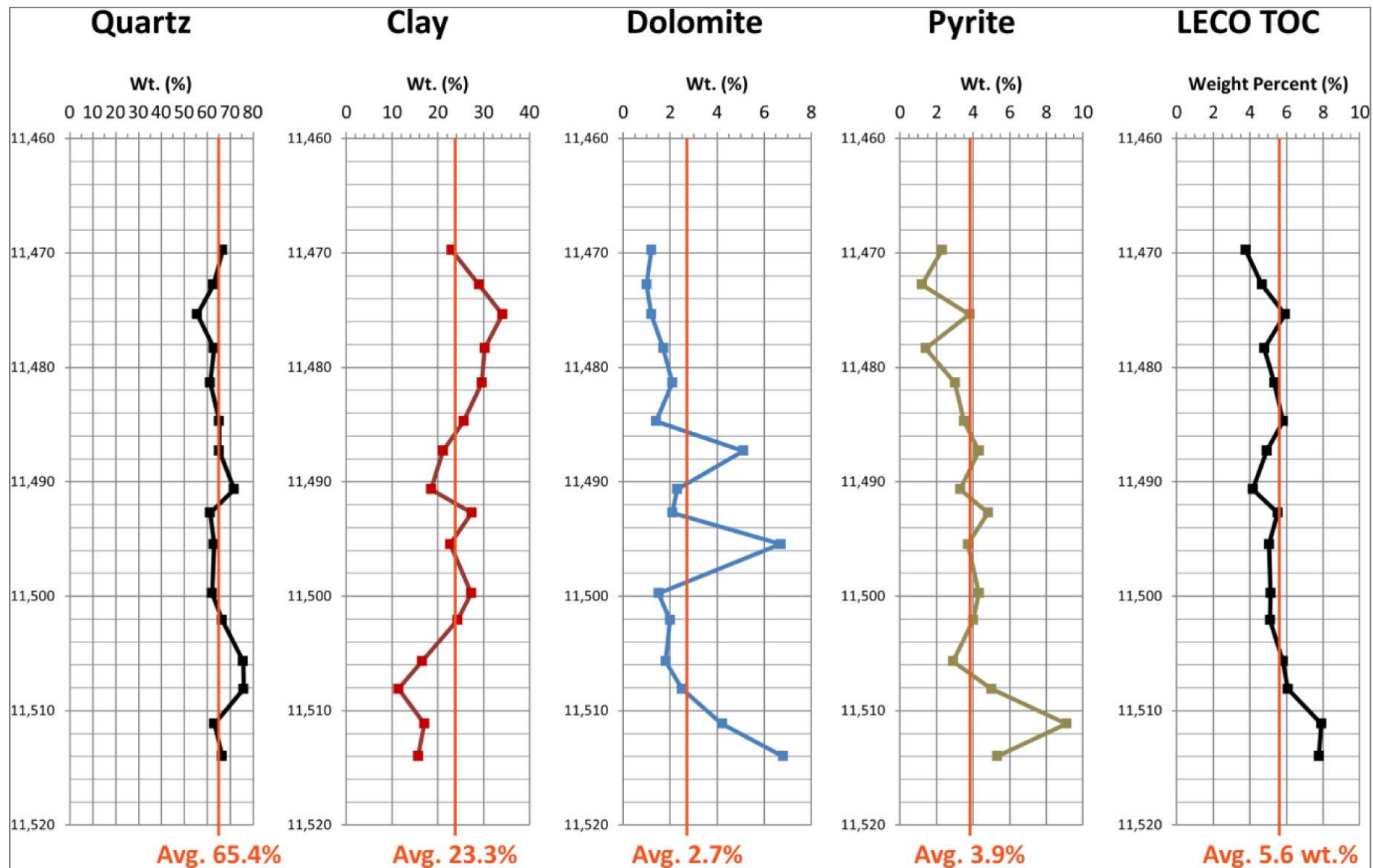


Figure 12. XRD and TOC data for the Woodford Shale core from the Hentz Family 7-1.

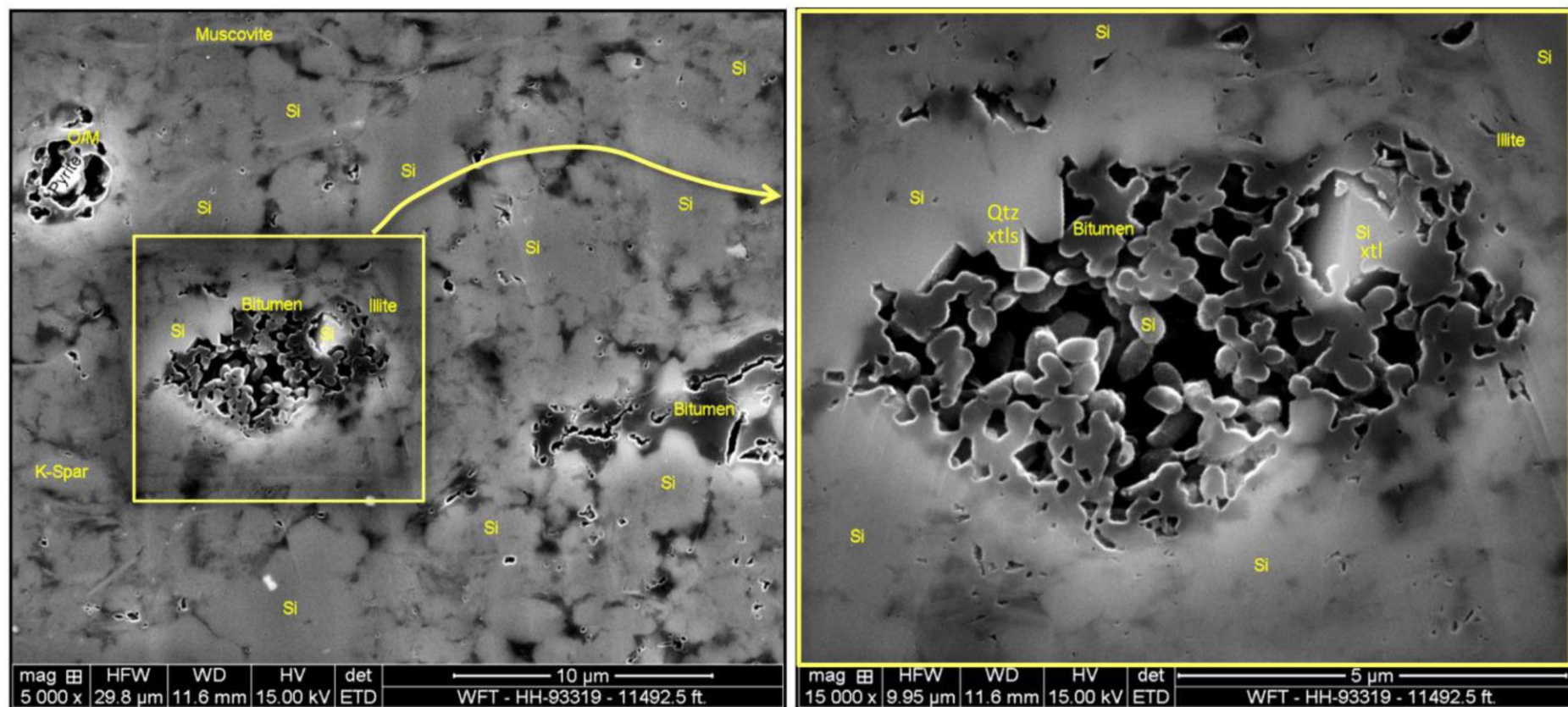


Figure 13. FE-SEM secondary electron image of an argon-ion milled surface, showing silica nanospheres at 15,000X magnification (modified from Drake et al., 2017).

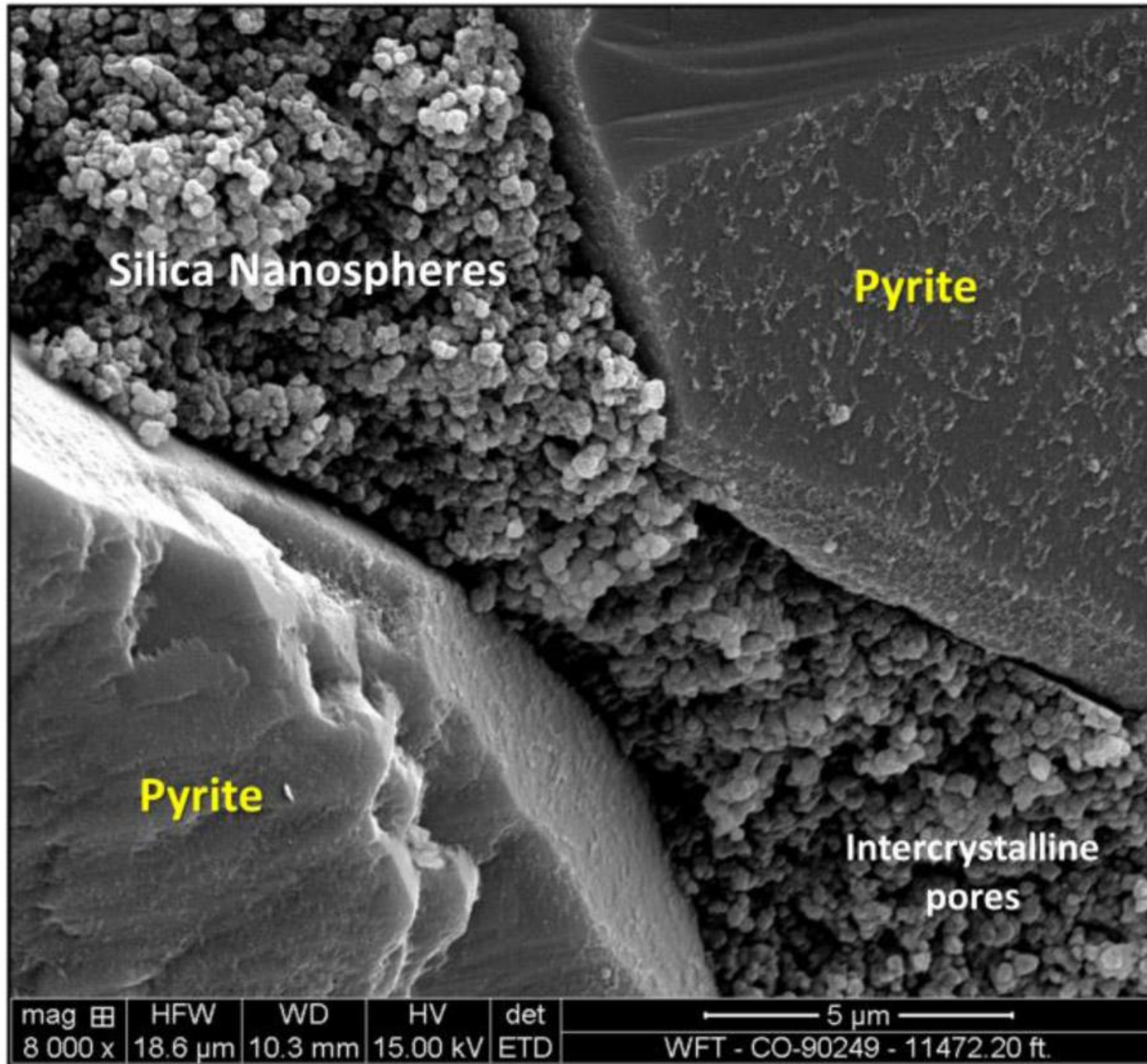


Figure 14. FE-SEM secondary electron image of a broken surface, showing silica nanospheres associated with pyrite at 8,000X magnification (modified from Drake et al., 2017).

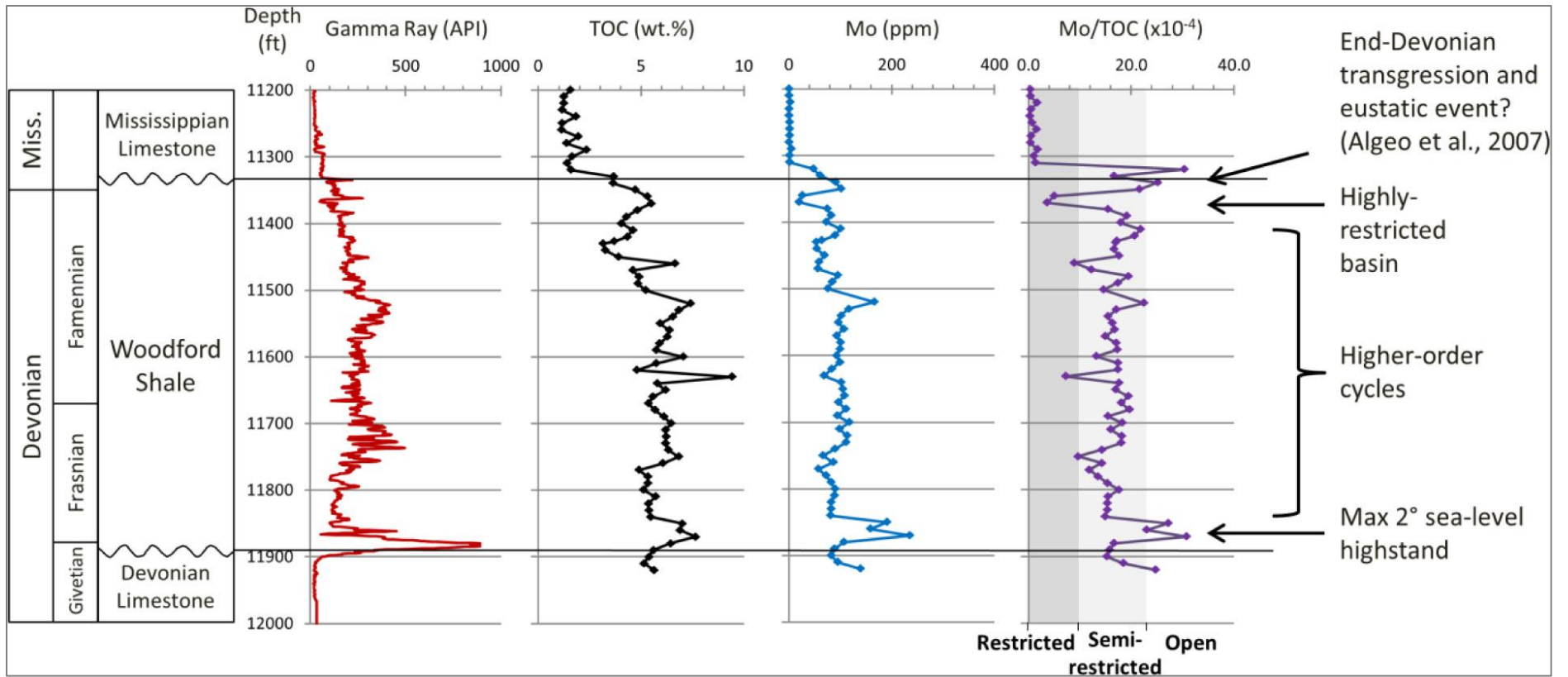


Figure 15. Gamma ray log, Mo and TOC concentrations from cuttings, and Mo/TOC for the entire Woodford section at the Hentz Family 7-1. Degrees of basin restriction (restricted, semi-restricted, and open) are from Algeo et al., 2007.

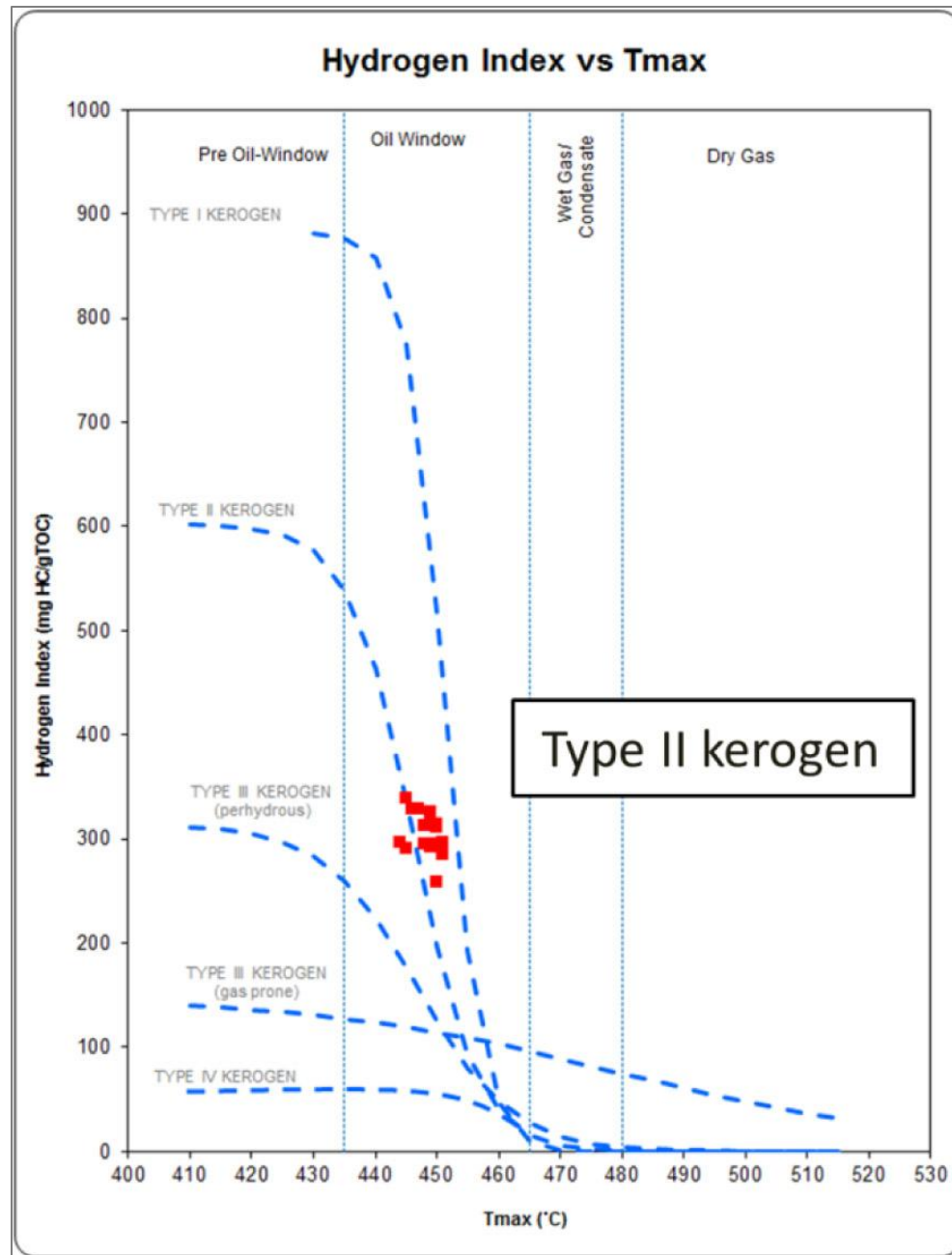


Figure 16. Hydrogen index (mg HC/gTOC) vs Tmax.

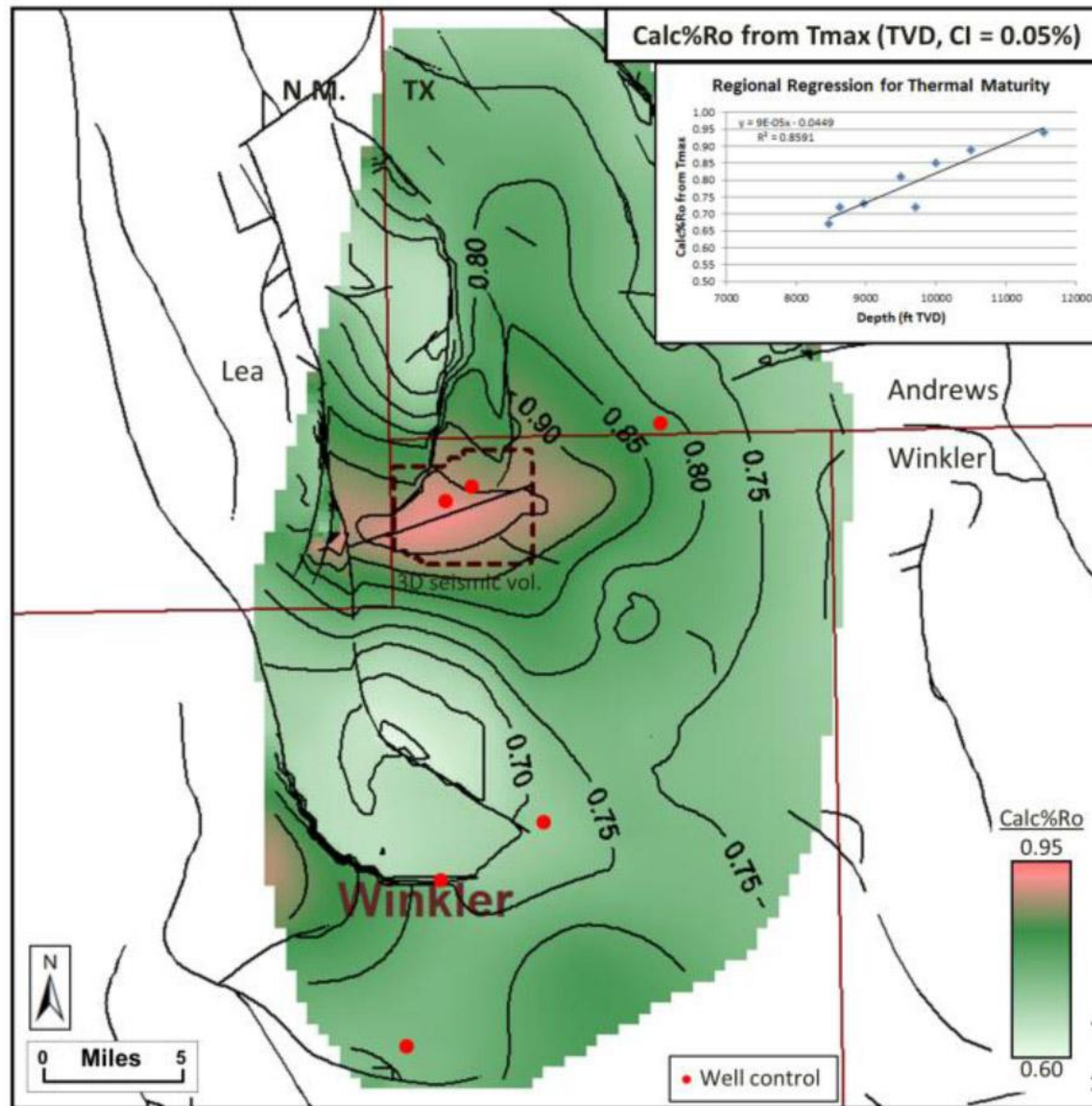


Figure 17. Regional thermal maturity map for the Woodford Shale. Calculated %Ro (Calc%Ro) from Tmax data (after Jarvie et al., 2001).

Tables:

Woodford Shale Core (Hentz Family 7-1)									
Samples	LECO TOC	S1 _{avg}	S2 _{avg}	S3 CO ₂ _{avg}	S3 CO _{avg}	Tmax _{avg}	HI _{avg}	OI _{avg}	PI _{avg}
no.	wt%	mg HC/g	mg HC/g	mg CO ₂ /g	mg HC/g	°C	S2x100/TOC	S3x100/TOC	S1/(S1+S2)
17	3.8-7.8	4.31	16.52	0.07	0.20	448	306	5.02	0.21

*after Jarvie

Table 1. Summary of key results from source rock analysis.

Woodford Shale Oil and Gas (Hentz Family 7-1)									
Samples	Type	API Grav.	wt% S	% Asph	Sat/Aro	wt% TOC	VREQ	Calc%Ro (avg)	VREG
2*	Oil (avg)	42.0	0.15	0.0	1.65		0.94		
4	Core Extract		0.3-0.4	1.6-2.3	0.7-0.9	3.8-7.6	0.93-0.94	0.91	
2	Gas (avg)								0.93

* Includes oil from adjacent horizontal well Bruce & Bar A55A56-2303 N 02WS, same Woodford landing zone

Table 2. Core-extract, oil, and gas analytical results. Abbreviations: Asph – asphaltenes, Sat – saturates, Aro – aromatics, VREQ – oil maturity from alkyl aromatic ratios, VREG – gas maturity from C2 and C3 isotopes.